Journal of Solid Mechanics Vol. 1, No. 3 (2009) pp. 213-225

Buckling Analysis of Simply-supported Functionally Graded Rectangular Plates under Non-uniform In-plane Compressive Loading

M. Mahdavian*

Department of Mechanical Engineering, Islamic Azad University, Arak Branch, Arak, Iran

Received 5 November 2009; accepted 24 November 2009

ABSTRACT

In this research, mechanical buckling of rectangular plates of functionally graded materials (FGMs) is considered. Equilibrium and stability equations of a FGM rectangular plate under uniform in-plane compression are derived. For isotropic materials, convergent buckling loads have been presented for non-uniformly compressed rectangular plates based on a rigorous superposition fourier solution for the in-plane Airy stress field and Galerkin's approach for stability analysis. The results for isotropic case will be compared with reference articles and finite element method (FEM) solution. Finally, the results will be achieved for a sample of FGM material as well as the research on the effect of power law index on buckling coefficient.

Keywords: Buckling; Airy stress; In-plane load; Functionally graded material

1 INTRODUCTION

STABILITY of plates is the most important classical subject well documented in numerous references and text books [1]. Most of the methods and analysis on buckling is related to uniform distribution load along the edges. But, in fact, the rectangular plates is usually the idealization of a small portion of a much larger and more complicated built-up plated structure and the applied loads are those exerted on the small portion by the adjoining structural elements. It is not easy to find out the actual distribution of the loads on boundary of the small rectangular portion under consideration because it requires modeling of the entire built-up structure. Thus, it is also necessary to examine the influence of various non-uniform load variations. In recent years, studies on new performance materials have addressed new materials known as functionally graded materials (FGMs). These are high performance heat resistant materials able to withstand ultra high temperature and extremely large thermal gradients used in aerospace industries. FGMs are microscopically inhomogeneous in which the mechanical properties vary smoothly and continuously from one surface to the other [2, 3]. Typically, these materials are made from a mixture of ceramic and metal. The nonlinear equilibrium equations and associated linear stability equations were expressed for bars, plates, and shells by Brush and Almorth in 1975 [4]. The subject matter of this book is the buckling behavior of structural members subjected to mechanical loads.

One case of un-uniform loading that has been studied reasonably well is that of compression by two collinear concentrated loads. Apart from the simplistic energy type analysis employed by Timoshenko [5] wherein the plane stress solution was completely obviated, there has been a more careful study based on finite element method to account for the steep in-plane stress gradients and the singular stresses directly under the points of loading [6]. The closely related case of uniform loading on a small portion of the edge usually called partial edge load or patch load has also been studied using a simplified approach [7] as well as rigorous series approach for plane stress analysis [8]. Except the above cases which are distinctly different from that of uniform loading applied all along the edge, general non-uniform loading has not received due attention in the literature till very recently. While early solutions

* *E-mail address:* mehdimahdaviyan@yahoo.com.

like that of Benoy [9] for a parabolically distributed uniaxial load can be cited, they suffer from drastic errors due to oversimplification. For instance, Benoy assumes that the parabolic stress distribution continues in the interior of the plate as well which is in total conflict with St.Venant's principle. A similar oversimplification of the in-plane stress solution, with a violation of the compatibility relations, is also found in a recent work [10] on orthotropic plates under parabolic load. The importance of a two-step procedure first to determine the in-plane stress field accurately, and second to determine the buckling load with due account of that stress field was clearly highlighted by Bert and Devarakonda [11] with reference to a sinusoidal distribution of the uniaxial load. Jana and Bhaskar [12] have employed a more rigorous series approach to study a wide variety of load distributions. In FGM case Nan et al. [13] directly address the constitutive relations of FGM and wish specifically used as an analytical approach to describe the uncoupled thermomechanical properties of metal/ceramic FGM. These noval materials were first introduced by a group of scientists in Sendai, Japan [14] and then rapidly developed by the scientists. Javaheri and Eslami presented the thermal and mechanical buckling of rectangular FGM plates based on the classical and high order plate theories [15]. The buckling analysis of circular FGM plates is given by Najafizadeh and Eslami [16]. A new way proposed recently for applying the boundary conditions is called the new version differential quadrature method (DQM) [17]. The method is successfully used to obtain the buckling loads for anisotropic plates with uniform in-plane loadings.

In the present article, the equilibrium and stability equations for FGMs are obtained on the basis of classical plate theory. Then the influence of different edge load distributions of a simply supported plate is examined. Analysis is very rapidly in this method and has ability to spread solution for any loading and boundary conditions. Once again, an analytical approach is adopted so as to lead to a set of standard results which will be useful for judging various numerical approaches commonly resorted to.

2 FUNCTIONALLY GRADED RECTANGULAR PLATES

FGM is typically made from a mixture of ceramics and metal or a combination of different metals. The ceramic constituent of the material provides the high temperature resistance due to its low conductivity. The ductile metal constituent, on the other hand, prevents fracture caused by stresses due to high temperature gradient in a very short period of time. Further, a mixture of a ceramic and a metal with continuously varying volume fraction can be easily manufactured. The volume fractions of the ceramic V_c and metal V_m corresponding to the power law are expressed [18] as

$$E(z) = E_c V_c + E_m (1 - V_c), \quad \nu(z) = \nu_\circ \tag{1}$$

where z is the thickness coordinate $\left(-h/2 \le h/2\right)$, h is the thickness of the plate and n is the power law index that takes values greater than or equal to zero. The variation of the composition of ceramics and metal is linear for n=1. The value of n equal to zero represents a fully ceramic plate. The mechanical properties FGM are determined from the volume fraction of the material constituents. We assume that the non-homogeneous material properties, such as the modulus of elasticity E change in the thickness direction z based on Voigt's rule over the whole range of the volume fraction [18]; while Poisson's ratio ν is assumed to be constant [20] as

$$V_c = \left(\frac{2z + h}{2h}\right)^p, \quad V_m = 1 - V_c \tag{2}$$

where subscripts m and c refer to metal and ceramic constituents, respectively. Substituting Eq. (1) into Eq. (2), material properties of the FGM plate are determined, which are the same as the equations proposed by Praveen and Reddy [18]:

$$E(z) = E_m + E_{cm}\left(\frac{2z + h}{2h}\right)^p, \qquad E_{cm} = E_c - E_m \tag{3}$$

$$(E_1, E_2, E_3) = \int_{-h/2}^{h/2} (1, z, z^2) E(z)\, \mathrm{d}z \tag{4}$$

3 EQUILIBRIUM AND STABILITY EQUATIONS

We initially consider an FGM rectangular thin flat plate ($-a/2 \le x \le a/2, -b/2 \le x \le b/2$ and thickness h) subjected to the mechanical loads. The general strain relations in the displacement z of middle plate are [4]

$$\begin{aligned} \bar{\in}_x &= \in_x + z k_x \\ \bar{\in}_y &= \in_y + z k_y \\ \bar{\in}_{xy} &= \in_{xy} + 2 z k_{xy} \end{aligned} \tag{5}$$

where ε_x and ε_y are the normal strain and ε_{xy} is the shear strain in middle plate. The strain- displacement relations are as

$$\begin{aligned} &\in_x = u_{,x} + \frac{1}{2}\beta_x^2,\ \in_y = v_{,y} + \frac{1}{2}\beta_y^2,\ \in_{xy} = (u_{,y} + v_{,x}) + \beta_x \beta_y, \\ &k_x = \beta_{x,x}, k_y = \beta_{y,y}, k_{xy} = \frac{1}{2}(\beta_{x,y} + \beta_{y,x}),\ \beta_x = -w_{,x},\ \beta_y = -w_{,y} \end{aligned} \tag{6}$$

Here u, v and w denote the displacement components in the x, y and z directions, respectively, and a comma indicates the partial derivative. Hook's law for plate is defined [22] are as

$$\begin{aligned} \bar{\sigma}_x &= \frac{E}{1-\nu^2}[\bar{\in}_x + \nu \bar{\in}_y] \\ \bar{\sigma}_y &= \frac{E}{1-\nu^2}[\bar{\in}_y + \nu \bar{\in} x] \\ \bar{\sigma}_{xy} &= \frac{E}{2(1+\nu)} \bar{\in}_{xy} \end{aligned} \tag{7}$$

The stress resultants N_{ij} , M_{ij} are expressed as

$$(N_{ij}, M_{ij}) = \int_{-h/2}^{h/2} \bar{\sigma}_{ij}\ (1, z)\, \mathrm{d}z \qquad i, j = x, y, xy \tag{8}$$

Substituting Eqs. (6) and (7) into Eqs. (8) give the constitutive relations are as

$$\begin{aligned} N_x &= \frac{E_1}{1-\nu_\circ^2}(\in_x + \nu_\circ \in_y) + \frac{E_2}{1-\nu_\circ^2}(k_x + \nu_\circ k_y) \\ N_y &= \frac{E_1}{1-\nu_\circ^2}(\in_y + \nu_\circ \in_x) + \frac{E_2}{1-\nu_\circ^2}(k_y + \nu_\circ k_x) \\ N_{xy} &= \frac{E_1}{2(1+\nu_\circ)} \in_{xy} + \frac{E_2}{1+\nu_\circ} k_{xy} \\ M_x &= \frac{E_2}{1-\nu_\circ^2}(\in_x + \nu_\circ \in_y) + \frac{E_3}{1-\nu_\circ^2}(k_x + \nu_\circ k_y) \\ M_y &= \frac{E_2}{1-\nu_\circ^2}(\in_y + \nu_\circ \in_x) + \frac{E_3}{1-\nu_\circ^2}(k_y + \nu_\circ k_x) \\ M_{xy} &= \frac{E_2}{2(1+\nu_\circ)} \in_{xy} + \frac{E_3}{1+\nu_\circ} k_{xy} \end{aligned} \tag{9}$$

The general equilibrium equations are obtained as

$$\begin{aligned} &N_{x,x}+N_{xy,y}=0\\ &N_{y,y}+N_{xy,x}=0\\ &M_{x,xx}+M_{y,yy}+2M_{xy,xy}-N_x\beta_{x,x}-N_y\beta_{y,y}-2N_{xy}\beta_{x,y}=0 \end{aligned} \tag{10}$$

Substituting Eq. (9) into Eq. (10) gives the constitutive relations are as

$$\frac{E_1}{1-\nu_\circ^2}(u_{,xx}+\nu_\circ v_{,yx})-\frac{E_2}{1-\nu_\circ^2}(w_{,xxx}+\nu_\circ w_{,yyx})+\frac{E_1}{2(1+\nu_\circ)}(u_{,yy}+v_{,xy})-\frac{E_2}{1+\nu_\circ}w_{,xyy}=0 \tag{11}$$

$$\frac{E_1}{1-\nu_\circ^2}(v_{,yy}+\nu_\circ u_{,xy})-\frac{E_2}{1-\nu_\circ^2}(w_{,yyy}+\nu_\circ w_{,xxy})+\frac{E_1}{2(1+\nu_\circ)}(u_{,yy}+v_{,xy})-\frac{E_2}{1+\nu_\circ}w_{,xyy}=0 \tag{12}$$

$$\begin{aligned} &\frac{E_2}{1-\nu_\circ^2}(u_{,xxx}+\nu_\circ v_{,yxx})-\frac{E_3}{1-\nu_\circ^2}(w_{,xxxx}+\nu_\circ w_{,yyxx})+\frac{E_2}{1-\nu_\circ^2}(v_{,yyy}+\nu_\circ u_{,xyy})\\ &-\frac{E_3}{1-\nu_\circ^2}(w_{,yyyy}+\nu_\circ w_{,xxyy})+\frac{E_2}{(1+\nu_\circ)}(u_{,yxy}+v_{,xxy})-\frac{2E_3}{1+\nu_\circ}w_{,xyxy}+N_{x\circ}w_{,xx}+N_{y\circ}w_{,yy}+2N_{xy\circ}w_{,xy}=0 \end{aligned} \tag{13}$$

Derivative Eq. (11) than x and Eq. (12) than y, then add them are as

$$\begin{aligned} &\frac{E_1}{1-\nu_\circ^2}(u_{,xxx}+\nu_\circ v_{,yxx})-\frac{E_2}{1-\nu_\circ^2}(w_{,xxxx}+\nu_\circ w_{,yyxx})+\frac{E_1}{1-\nu_\circ^2}(v_{,yyy}+\nu_\circ u_{,xyy})\\ &-\frac{E_2}{1-\nu_\circ^2}(w_{,yyyy}+\nu_\circ w_{,xxyy})+\frac{E_1}{(1+\nu_\circ)}(u_{,yxy}+v_{,xyx})-\frac{2E_2}{1+\nu_\circ}w_{,xyxy}=0 \end{aligned} \tag{14}$$

To multiply Eq. (14) at E_2 and substituting into Eq. (13) gives as

$$\begin{aligned} &\frac{E_2^2}{E_1(1-\nu_\circ^2)}(w_{,xxxx}+\nu_\circ w_{,yyxx})+\frac{E_2^2}{E_1(1-\nu_\circ^2)}(w_{,yyyy}+\nu_\circ w_{,xxyy})+\frac{2E_2^2}{E_1(1+\nu_\circ)}w_{,xyxy}\\ &-\frac{E_1E_3}{E_1(1-\nu_\circ^2)}(w_{,xxxx}+\nu_\circ w_{,yyxx})-\frac{E_1E_3}{E_1(1-\nu_\circ^2)}(w_{,yyyy}+\nu_\circ w_{,xxyy})-\frac{2E_1E_3}{E_1(1+\nu_\circ)}w_{,xyxy}\\ &+N_{x\circ}w_{,xx}+N_{y\circ}w_{,yy}+2N_{xy\circ}w_{,xy}=0 \end{aligned} \tag{15}$$

At long last, gives the constitutive relations are as

$$\frac{E_2^2-E_1E_3}{E_1(1-\nu_\circ^2)}\nabla^4 w+N_{x\circ}w_{,xx}+N_{y\circ}w_{,yy}+2N_{xy\circ}w_{,xy}=0 \tag{16}$$

For derived stability equations, virtual displacements are defined [23] as

$$u=u_\circ+u_1,\ v=v_\circ+v_1,\ w=w_\circ+w_1 \tag{17}$$

Results in the stability equations are as

$$\frac{E_2^2-E_1E_3}{E_1(1-\nu_\circ^2)}\nabla^4 w_1+N_{x\circ}w_{1,xx}+N_{y\circ}w_{1,yy}+2N_{xy\circ}w_{1,xy}=0 \tag{18}$$

The subscript 1 refers to the state of stability and subscript 0 refers to the state of equilibrium. The terms N_{xo} , N_{yo} and N_{xyo} are buckling force resultants obtained from the linear equilibrium Eqs (11), (12) and (13).

4 FORMULATION AND ANALYSIS

A simply supported rectangular plate ($-a/2 \le x \le a/2, -b/2 \le x \le b/2$ and thickness h) subjected to compressive loading in the x direction is considered. The load distributions are symmetrical about the mid-edges so that their net effect is to simply compress the plate without any overall bending action; further the distributions are identical on opposite edges.

4.1. In-plane stress analysis

The first step is to obtain the internal plane stress field corresponding to any applied loading on the edges. This requires a solution of the two-dimensional elasticity problem governed by the biharmonic differential equation

$$\frac{\partial^4 \varphi}{\partial x^4} + 2\frac{\partial^4 \varphi}{\partial x^2 \partial y^2} + \frac{\partial^4 \varphi}{\partial y^4} = 0 \tag{19}$$

where φ is Airy's stress function. A rigorous solution of this equation, satisfying the boundary conditions on all the edges of the plate, can be obtained by superposition of two building blocks as shown in Fig. 1, each building block having a stress function in the form of Fourier series [21]. The first building block corresponds to the applied compressive load on the edges $x = \pm a/2$, with the coordinate system placed at the center of the plate is loaded with the in-plane loading as

$$\sigma_x = -\sigma_0 \cos\left(\frac{\pi y}{b}\right) \tag{20}$$

Substituting the Airy stress function ϕ_1 given by

$$\phi_1 = f(x)\cos\left(\frac{\pi y}{b}\right) \tag{21}$$

Into governing differential equation $\nabla^4 \phi = 0$, one can obtain the general solution for the functional $f(x)$ as

$$f(x)^{(4)} - 2\left(\frac{\pi^2}{b^2}\right) f(x)^{(2)} + \left(\frac{\pi}{b}\right)^4 f(x) = 0 \tag{22}$$

In which C_1 through C_4 are constants which are to be obtained from the boundary conditions. It is to be noted that the stress function solution as given by Eqs. (21) and (22) gives a zero normal stress at $y = \pm b/2$ edges. Substituting the zero shear stress boundary condition as well as the normal stress distribution as defined in Eq. (21), at the edges $x = \pm a/2$, yield a complete solution for the in-plane stress. (See Appendix A for complete solution)

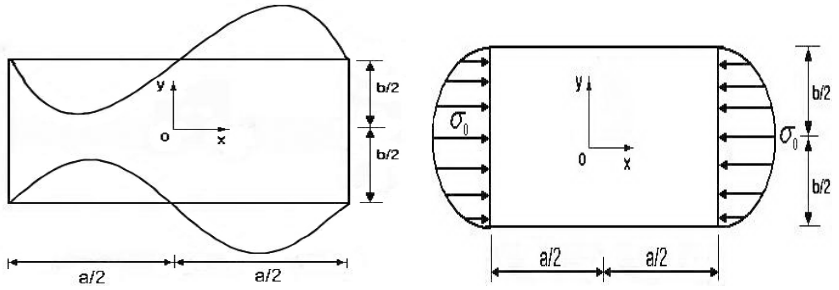

Fig.1
The building blocks required for compression.

$$\phi_1 = \left[C_1 \cosh\left(\frac{\pi x}{b}\right) + C_4 x \sinh\left(\frac{\pi x}{b}\right) \right] \cos\left(\frac{\pi y}{b}\right) \tag{23}$$

But, the above in-plane stress solution gives a residual shear stress distribution at the $y = \pm b/2$ edges, it is given by

$$\tau_1 \Big|_{y=\frac{b}{2}} = \left(\frac{\pi}{b}\right) \left[\left(C_1 \left(\frac{\pi}{b}\right) + C_4 \right) \sinh\left(\frac{\pi x}{b}\right) + C_4 \left(\frac{\pi x}{b}\right) \cosh\left(\frac{\pi x}{b}\right) \right] \tag{24}$$

In the present problem, a solution consisting of two superposed stress functions is sufficient to satisfy the required boundary conditions accurately. In order to eliminate these shear stresses at four edges, a building block is necessary. It is shown in Fig. 1 and corresponds to shear stresses applied along $y = \pm b/2$, and taken as

$$\phi_2 = \sum_{m=1,2,} f(y) \cos\left(\frac{2m\pi x}{a}\right) \tag{25}$$

It is to be observed that whereas the initial stress-function solution (ϕ_1) is a one-term solution, the second stress-function solution (ϕ_2) is a series solution. However, at the most, the first three or four series terms are sufficient to obtain a close approximation for the residual shear stress distribution due to ϕ_1. Although the stress-function solution ϕ_2 has zero normal stresses at the $y = \pm b/2$ edges and zero shear stresses at $x = \pm a/2$ edges, it does produce a residual normal stress (σ_x). However, it is observed that this σ_x stress distribution is once again sinusoidal with a very small magnitude. Consequently, a renormalization of the superposed σ_x distribution has to be carried out such that the resulting σ_x stresses are very nearly as specified by Eq. (20). This renormalization is carried out using a small uniform stress and a multiplication factor. This methodology gives good results as shown in the net section. For (ϕ_2) into governing differential equation $\nabla^4 \phi = 0$, one can obtain the general solution for the functional $f(y)$ as

$$f(y) = D_{1m} \cosh\left(\frac{2m\pi y}{b}\right) + D_{2m} \sinh\left(\frac{2m\pi y}{b}\right) + D_{3m} y \cosh\left(\frac{2m\pi y}{b}\right) + D_{4m} y \sinh\left(\frac{2m\pi y}{b}\right) \tag{26}$$

Imposing the zero normal stress boundary condition at the $y = \pm b/2$ edges, an interrelation between D_{1m} and D_{4m} can be obtained. Now superposition of the shear stress distribution at the $y = \pm b/2$ edges and equating the resultant to zero yields a complete solution, as

$$\begin{aligned} &\sigma_{y\,2} \Big|_{y=b/2} = 0 \\ &(\tau_{xy\,2+} \tau_{xy\,1}) \Big|_{y=b/2} = 0 \end{aligned} \tag{27}$$

The final solution is

$$\phi_2 = \sum_{m=1,2} \left[D_{1m} \cosh\left(\frac{2m\pi y}{b}\right) + D_{4m} y \sinh\left(\frac{2m\pi y}{b}\right) \right] \cos\left(\frac{2m\pi x}{a}\right) \tag{28}$$

where the constants are as defined in the Appendix B. Fig. 2 shows the comparative shear stresses at $y = \pm b/2$ plate edges for the case of ϕ_1 stress function solution only and the superposed $((\phi_1 + \phi_2))$ stress function solution. From this figure, one can clearly see that the superposed solution satisfied the zero shear stress boundary condition (on all four edges) very accurately.

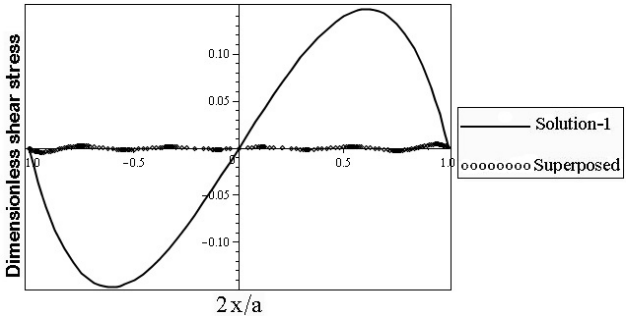

Fig. 2
Dimensionless shear stress ((τ_{xy}/σ_0)) distribution at ($(2y/b = \pm 1)$) edges (aspect ratio $a/b = 1$) (solution-1 corresponds the stress function solution ϕ_1 and superposed solution is the total($(\phi_1 + \phi_2)$) solution).

4.2. Analysis for stability

The governing differential equation for thin plate buckling is

$$\nabla^4 w + \frac{h}{D}(\sigma_x \frac{\partial^2 w}{\partial x^2} + 2\tau_{xy} \frac{\partial^2 w}{\partial x \partial y} + \sigma_y \frac{\partial^2 w}{\partial y^2}) = 0 \tag{29}$$

where *D* is the flexural rigidity, *h* is the plate thickness, and *w* is the normal deflection. The well-known Airy stress function are defined as

$$\phi = \phi_1 + \phi_2$$
$$\sigma_x = \frac{\partial^2 \phi}{\partial y^2}, \sigma_y = \frac{\partial^2 \phi}{\partial x^2}, \tau_{xy} = -\frac{\partial^2 \phi}{\partial x \partial y} \tag{30}$$

Owing to the complexity of the resulting plate buckling equation when each of the in-plane stress is a series sum, exact analytical solution may not be possible. Therefore, the buckling solution is obtained by using the Galerkin method for the case of simply supported rectangular plates. For the present case of simply supported rectangular plates with central coordinate system, the trial functions are

$$w(x, y) = w_0 \cos(\frac{m\pi x}{a}) \cos(\frac{n\pi y}{b}), \qquad \{m, n = 1, 3, 5, ...\} \tag{31}$$

As is well known, the critical loads obtained by seeking non-trivial solutions of the homogenous system of equations is given by

$$\iint R \cos(\frac{m\pi x}{a}) \cos(\frac{n\pi y}{b}) \, dx \, dy = 0 \tag{32}$$

where *R* is the residual obtained by substitution of the assumed *w* in the left-hand side of Eq. (29). Numerical calculations were conducted using symbolic math package Mathamatica (version 6.0)
All the load distributions shown in Fig. 3 are considered for compression load.

5 RESULTS AND DISCUSSION

5.1. Isotropic plate

Further, all the plates are taken to be of square plan-form. The first step is to examine the correctness of the superposition approach employed for plane stress analysis. Numerical results are compared for convergence between three-term Galerkin solution and four-term solution. Some representative results for Sinusoidal load is presented in Table 1. Although the results obtained by Benoy [9] are for the case of parabolic loading, one can

compare the solutions due to the close similarity of sinusoidal and parabolic stress distributions, and are compared with finite element program ANSYS 10. The plate width, plate thickness, Young's modulus and Poisson's coefficient were kept constant in the parameter study: b=100 mm, h=0.7 mm, E=210 000 N/mm^2, v=0.3, a/b=1. In the model elements Shell98 8-Node Structural were used, based in Mindlin plate theory. The mesh density for each plate was 40×40 elements.

5.2. FGM plate

To illustrate the proposed approach, a ceramic-metal FGM is considered. The combination of materials consists of aluminum and alumina. The Young's modulus and Poisson's ratio for aluminum are E_m = 70 Gpa, v_m = 0.3 and for alumina are E_c = 380 Gpa, v_c = 0.3. Note that Poisson's ratio is selected to be constant and equal to 0.3. The convergent net buckling load for different distributions is shown in Table 2. One should note from Tables 1 and 2 that the effect of a non-uniform load distribution is quite significant. Variation of the critical buckling coefficient K_{cr} versus the volume p are listed in Table 3. In this Table, the values of critical buckling coefficients K_{cr} is obtained by the method developed in the present article. This table shows that the critical buckling coefficient increases with the increase of the power law index p. It is interesting to note that the critical buckling coefficients for FGM plates (p>1) are considerably higher than isotropic plates (p = 0).

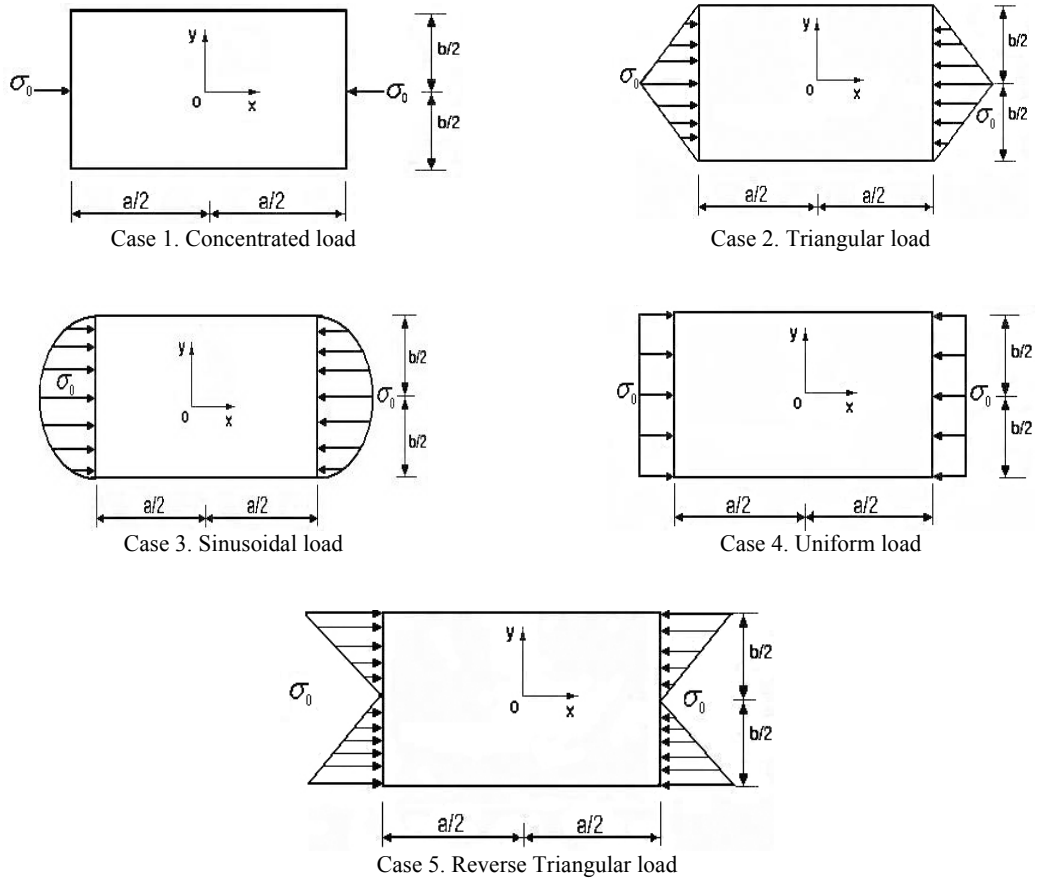

Fig. 3
Various load distributions considered.

Table 1

Sinusoidal buckling load (values for K in $P_{cr} = K\pi^2 D / b$) for an isotropic square plate and simply supported edges (v = 0.3)

a/b	Present (Superposition)	DQM [17]	FEM Solution, ANSYS	Benoy [9]	Van Der Neut [24]
1	5.149	5.408	5.286	4.59	4.68

Table 2

Total buckling coefficient (Values for K in $P_{cr} = K\pi^2 D / b$) for an isotropic square plate and simply supported edges ($\nu = 0.3$)

Load distribution	Present (Superposition)	FEM Solution, ANSYS
Concentrated load	2.409	2.582
Triangular load	3.540	3.315
Uniform load	4	3.972
Reverse Triangular Load	4.69	4.81
Sinusoidal load	5.149	5.286

Table 3

Total buckling coefficient (GN) for FGM square plate and simply supported edges with various p (power law index)

P	Concentrated load	Triangular load	Uniform load	Reverse Triangular load	Sinusoidal load
1	4.015	5.901	6.666	7.77	8.581
2	14.729	21.645	24.452	28.45	31.477
3	29.855	43.873	49.562	57.67	63.801
4	49.086	72.134	81.487	94.81	104.898
5	72.376	106.359	120.151	139.81	154.669
6	99.723	146.547	165.551	192.632	213.111
7	131.137	192.711	217.699	253.31	280.242
8	166.625	244.861	276.613	321.862	356.080
9	206.194	303.009	342.301	398.295	440.630
10	249.859	367.162	414.773	482.623	533.932
11	297.597	437.328	494.037	574.853	635.968
12	349.438	513.511	580.099	674.994	746.755
13	405.378	595.716	672.964	783.049	866.298
14	465.417	683.946	772.635	899.025	994.603
15	529.558	778.204	879.115	1022.92	1131.674

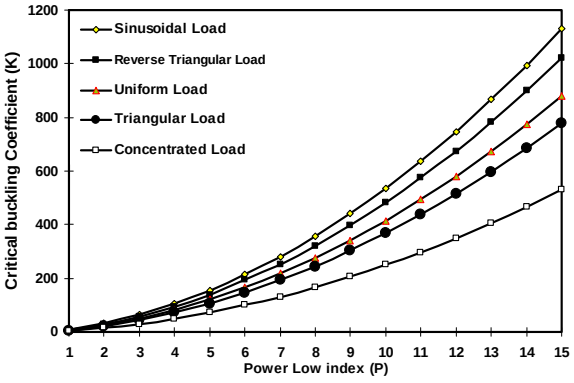

Fig. 4
Buckling coefficient K_{cr} of FGM square plate, for simply supported edges, for various load distributions and for various values of power law index.

Fig. 4 shows the critical buckling coefficients K_{cr} for various load distributions and for various values of power law index $(a/b = 1)$. It is seen that the critical buckling coefficients increases with the increase of power law index. Figs 5, 6, 7, and 8 are graphs that show the critical buckling coefficients K_{cr} increases with the increase of aspect ratio (a/b) for the cases of concentrated, sinusoidal, triangular and reverse triangular compression load with simply supported boundary conditions, respectively.

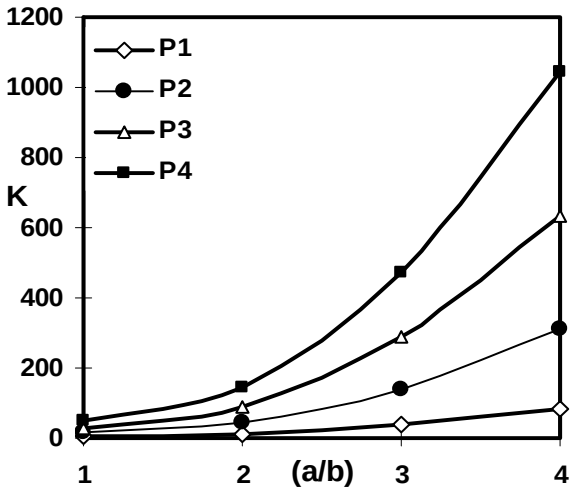

Fig. 5
K_{cr} of FGM rectangular plate under Concentrated Load, for various values of power law index and for various values of aspect ratio (*a/b*).

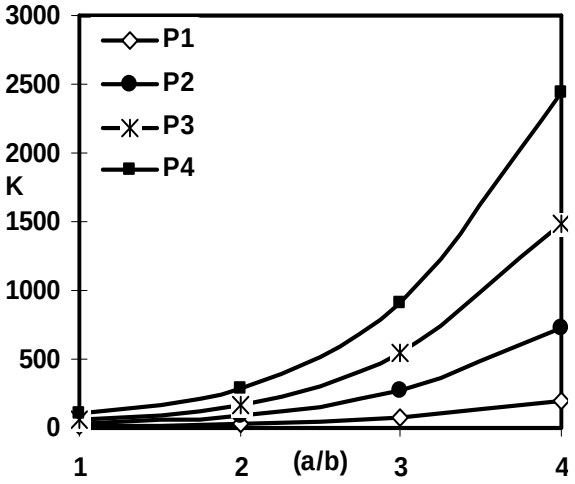

Fig. 6
K_{cr} of FGM rectangular plate under Sinusoidal Load, for various values of power law index and for various values of aspect ratio (*a/b*).

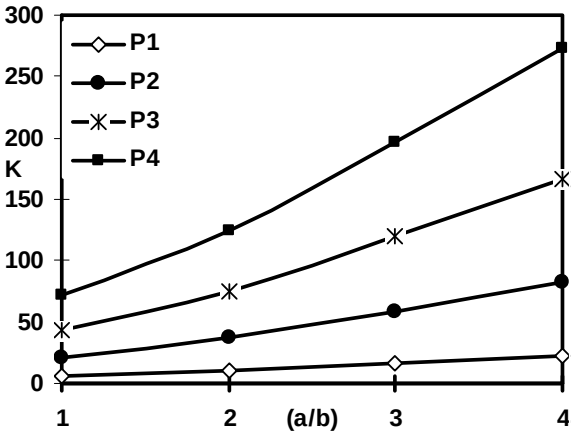

Fig. 7
K_{cr} of FGM rectangular plate under Triangular Load, for various values of power law index and for various values of aspect ratio (*a/b*).

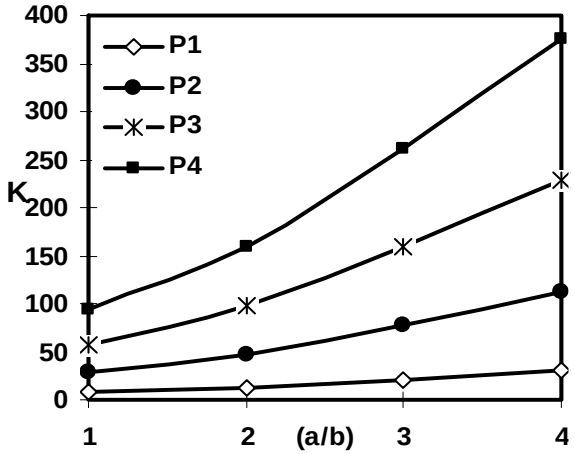

Fig. 8
K_{cr} of FGM rectangular plate under Re-Triangular Load, for various values of power law index and for various values of aspect ratio (*a/b*).

6 CONCLUSION

In the present article, convergent buckling loads have been presented for non-uniformly compressed rectangular plates based on a rigorous superposition Fourier solution for the in-plane stress field and Galerkin's approach for stability analysis. Then, the equilibrium and stability equations for functionally graded rectangular plates are obtained with the assumption of power law composition for the constituent materials. Buckling analysis of FGM plate under various load distributions is presented. It is concluded that:

1. For such cases, the effect of non-uniform distribution is to significantly alter the critical value of the total load, and such changes are much more than the corresponding isotropic plate. Further, depending on the nature of the load distribution, the buckled configuration may also change.
2. The critical buckling coefficients K_{cr} for the isotropic plate is generally lower than the FGM rectangular plate.
3. The critical buckling coefficients K_{cr} for the FGM rectangular plate is increased by increasing the aspect ratio (a/b).
4. The critical buckling coefficients K_{cr} for the FGM rectangular plate is increased by increasing the volume power law index p.
5. The present converged analytical results will be useful for judging the accuracy of various approximate methods commonly employed.

APPENDIX

Appendix A

The constants occurring in the stress function ϕ_1 equations are:

Eq. (23): $$C_1=\left(\frac{\sigma_0 b^2}{\pi^2}\right)\left[\frac{\sinh\left(\frac{\pi a}{2b}\right)+\left(\frac{\pi a}{2b}\right)\cosh\left(\frac{\pi a}{2b}\right)}{\sinh\left(\frac{\pi a}{2b}\right)\cosh\left(\frac{\pi a}{2b}\right)+\left(\frac{\pi a}{2b}\right)}\right], \qquad C_4=\left(\frac{-\sigma_0 b^2}{\pi^2}\right)\left[\frac{-\left(\frac{\pi}{b}\right)\sinh\left(\frac{\pi a}{2b}\right)}{\sinh\left(\frac{\pi a}{2b}\right)\cosh\left(\frac{\pi a}{2b}\right)+\left(\frac{\pi a}{2b}\right)}\right]$$

Appendix B

The constants occurring in the stress function ϕ_2 equations are:

$$\text{Eq. (28):}\quad D_{1m}=\left[\frac{-\tau_1 a^2\sin\left(\frac{2m\pi x}{a}\right)}{4m^2\pi^2\left(\left(1-\frac{a}{bm\pi\tanh\left(\frac{m\pi b}{a}\right)}\right)\sinh\left(\frac{m\pi b}{a}\right)-\frac{\cosh\left(\frac{m\pi b}{a}\right)}{\tanh\left(\frac{m\pi b}{a}\right)}\right)}\right]$$

$$D_{4m}=\left(\frac{1}{b\tanh\left(\frac{m\pi b}{a}\right)}\right)\left[\frac{2\tau_1 a^2\sin\left(\frac{2m\pi x}{a}\right)}{4m^2\pi^2\left[\left(1-\frac{a}{bm\pi\tanh\left(\frac{m\pi b}{a}\right)}\right)\sinh\left(\frac{m\pi b}{a}\right)-\frac{\cosh\left(\frac{m\pi b}{a}\right)}{\tanh\left(\frac{m\pi b}{a}\right)}\right]}\right]$$

REFERENCES

[1] Bulson P.S., 1970, *The Stability of Flat Plates*, Chatto and Windus, London.

[2] Yamanouchi M, Koizumi M., 1991, Functionally gradient materials, in: *Proceeding of the first international symposium on functionally graded materials*, Sendai, Japan.

[3] Fukui Y., 1991, Fundamental investigation of functionally graded materials, manufacturing system using centrifugal force, *Japan Society of Mechanical Engineering, International Journal Series III* **34**(1): 144-148.

[4] Brush D.O., Almroth B.O., 1975, *Buckling of Bars, Plates and Shells*, McGraw-Hill, New York.

[5] Timoshenko S.P., Gere J.M., 1961, *Theory of Elastic Stability*, McGraw-Hill, New York.

[6] Leissa A.W., Ayoub E.F., 1988, Vibration and buckling of a simply supported rectangular plates subjected to a of in-plane concentrated forces, *Journal of Sound and Vibration* **127**: 155-171.

[7] Khan M.Z., Walker A.C., 1972, Buckling of plates subjected to localized edge loading, *Engineering* **50**: 225-232.

[8] Baker G., Pavlovic M.N., 1982, Elastic stability of simply supported rectangular plates under locally edge forces, *ASME Transaction*, *Journal of Applied Mechanics* **49**: 177-179.

[9] Benoy M.B., 1969, An energy solution for the Buckling of rectangular plates under non-uniform in-loading, *Aerospace Journal* **73**: 974-977.

[10] Hu H., Badir A., Abatan A., 2003, Buckling behavior of a graphite/epoxy composite plate under parabolic variation of axial loads, *International Journal of Mechanical Sciences* **45**: 1132-1147.

[11] Bert C.W., Devarakonda K.K., 2003, Buckling of rectangular plate subjected to nonlinearly distributed in-plane loading, *International Journal of Solids and Structures* **40**: 4097-4106.

[12] Jana P., Bhaskar K., 2004, Buckling of rectangular plates under non-uniform compression using rigorous plane stress solution, in: *Proceedings of the International Conference on Theoretical, Analytical, Computational and Experimental Mechanics*, IIT Kharagpur, 28-30 December.

[13] Nan C.W., Yuan R.Z., Zhang L.M., 1993, The physics of metal/ceramic functionally gradient materials, *Ceramic Transactions, Functionally Gradient Materials* **34**: 75-82.

[14] Koizumi M., 1997, FGM Activities in Japan, *Composite Part B: Engineering* **28**(1-2): 1-4.

[15] Javaheri R., Eslami M.R., 2002, Thermal buckling of graded plates based on higher order theory, *Journal of Thermal Stresses* **25**(7): 603-625.

[16] Najafizadeh M.M., Eslami M.R., 2002, Buckling analysis of circular of functionally graded materials under uniform redial compression, *International Journal of Mechanical Sciences* **4**(12): 2479-2493.

[17] Wang X., Tan M., Zhou Y., 2003, Buckling analyses of anisotropic plates and isotropic skew plates by the new version differential quadrature method, *Thin-Walled Structure* **41**: 15-29.

[18] Praveen G.N., Reddy J.N., 1998, Nonlinear transient thermoelastic analysis of functionally graded ceramic-metal plates, *International Journal of Solids and Structures* **35**(33): 4457-4476.

[19] Wetherhold R.C., Seelman S., Wang J., 1996, The use of functionally graded materials to eliminate or control thermal deformation, *Composites Science and Technology* **56**: 1099-1104.

[20] Tanigawa Y., Morishita H., Ogaki S., 1999, Derivation of system of fundamental equations for a three dimensional thermoelastic field with nonhomogeneous material properties and its application to a semi-infinite body, *Journal of Thermal Stresses* **22**: 689-711.
[21] Timoshenko S.P., Goodier J.N., 1970, *Theory of Elasticity*, McGraw-Hill, New York.
[22] Ugural A.C., 1981, *Stress in Plate and Shells*, McGraw-Hill, New York.
[23] Reddy J.N., 2000, Analysis of functionally graded plates, *International Journal of Numerical Methods in Engineering* **47**: 663-684.
[24] Van der Neut A., 1958, Buckling caused by thermal stresses, In: *High temperature effects in aircraft structures*, AGARD report **28**: 215-247.